A Compact and Miniaturized Broadband Phase Shifter Using Coupled-lines

Yongle Wu[*], Siyue Zhou, Xiaochuan Shen, and Yuanan Liu

School of Electronic Engineering, Beijing Key Laboratory of Work Safety Intelligent Monitoring
Beijing University of Posts and Telecommunications, P.O. Box. 282, 100876, Beijing, China
wuyongle138@gmail.com[*], zsy.amanda@gmail.com, shenxc188@gmail.com, yuliu@bupt.edu.cn

Abstract ─ In this paper, a compact and miniaturized broadband phase shifter using coupled-lines (CL) is proposed. This broadband phase shifter merely consists of two sections, one pair of CL as the reference and another two parallel CLs as the main body. An analysis of even-odd mode on the theoretical circuit is shown to explain the basic principle of the proposed phase shifter. For demonstration of this novel configuration, a broadband 90° phase shifter was designed and fabricated. The measured results present that the proposed phase shifter can provide a stable wide bandwidth (over 80%) of 90° phase difference with deviation less than 6.7°, good return losses more than 10 dB and low insertion losses less than 0.53 dB.

Index Terms ─ Broadband, coupled-line (CL), phase shifter.

I. INTRODUCTION

Differential phase shifter is a key component to various communication systems. It is often designed as a four-port passive component comprised of two paths, the main body for phase delay and the reference section for phase adjustment. There are two phase shifts: $\angle S_{21}$ from reference part, and $\angle S_{43}$ from main body. The purpose of this configuration is to create a stable phase difference between the two sections, namely $\Delta\Phi = \angle S_{43} - \angle S_{21}$, over a wide bandwidth. The values of shifted phase rely on the different circuit parameters of the differential phase shifter.

The classic Schiffman phase shifter in [1, 2] achieved an 80% of bandwidth with a phase error of 10°. From then on, a serial of designs aimed at broadening the bandwidth with lower phase deviation were proposed. One approach by adding a T-shaped open stub on the main line was invented in [3], which yielded a wide bandwidth of 82% and phase inaccuracy of 6.4°. Based on these designs, the reference part was developed with some parallel multi-section coupled-lines in [4]. Another structure utilized multi-section radial stubs on the main line [5], which leads to an ultra-wideband frequency with a phase deviation of 9.02°. In addition, the multi-layer structure used broadside-coupled microstrip patches [6], achieving various shifted phase ranging from -180° to 180°. On the other hand, a T-type bandpass network for the main body merely depending on the L/C components was designed in [7]. It accomplished a better bandwidth larger than 125%. However, the circuits in [3-6] often require a complicated technique of fabrication, especially the multi-layer structure which is not suitable for the single-layer components. Meanwhile, the L/C components in [7] limit the performance when operating at a higher frequency.

This paper proposes a novel broadband phase shifter using ***coupled-lines*** with a ***compact*** structure. A theoretical model was analyzed via even-odd mode and kinds of circuit parameters for different shifted phase were provided and simulated as well. For experimental validations, an example of a broadband 90° phase shifter was simulated, fabricated, and measured.

II. PHASE SHIFTER DESIGN

The schematic of the proposed differential phase shifter with four ports is shown in Fig. 1 (a). It contains two paths: Path 1 employs only one coupled-line with an interconnected point as the reference section; Path 2 utilizes two pair of parallel CLs as main body.

Compared to the previously reported phase shifters, the circuit of this novel phase shifter is compact and miniaturized since it simply consists of some coupled-lines maintaining wide-band feature. Besides, this main body includes two connected sections with one connecting point shorted to ground by two vias. The electrical parameters of the ideal circuit are defined as follow: the even-mode and odd-mode characteristic impedances are Z_{ei} and Z_{oi} ($i = 1, 2, 3$), respectively; while, θ_j ($j = 1, 2$) corresponds to the electrical lengths of the reference part and the main body. The electrical lengths θ_j ($j = 1, 2$) at the frequency f are defined as:

$$\theta_1 = \theta_{1o}\frac{f}{f_0}, \qquad \theta_2 = \theta_{2o}\frac{f}{f_0}, \qquad (1)$$

where θ_{jo} ($j = 1, 2$) are the electrical lengths of the reference part and the main body at the designed frequency f_0. In addition, Z_0 stands for the characteristic impedance of each port.

Since the topology of the schematic is symmetric, as illustrated in Fig. 1 (a), it means that the theoretical

analysis can be simplified with the even-odd mode method displayed in [8]. Figure 1 (b) and Fig. 1 (c) present the symmetric equivalent circuits of the main body (Path 2) when separately motivated by even-mode source or odd-mode source.

As for the Fig. 1 (b) and Fig. 1 (c), the input impedances of the Path 2 both for the even- and odd-mode equivalent circuits can be expressed as:

$$Z_{ine} = \frac{Z_{e2}Z_{e3}}{j[Z_{e3}\tan(\theta_2)-Z_{e2}\cot(\theta_2)]}, \quad (2a)$$

$$Z_{ino} = -\frac{Z_{o2}Z_{o3}\tan(\theta_2)}{j(Z_{o3}+Z_{o2})}. \quad (2b)$$

Based on the Equations (2a) and (2b), the reflection coefficients of the Path 2 for each mode excitations S_{33e} and S_{33o} can be obtained by:

$$S_{33e} = \frac{Z_{ine}-Z_0}{Z_{ine}+Z_0}$$
$$= \frac{Z_{e2}Z_{e3}-jZ_0[Z_{e3}\tan(\theta_2)-Z_{e2}\cot(\theta_2)]}{Z_{e2}Z_{e3}+jZ_0[Z_{e3}\tan(\theta_2)-Z_{e2}\cot(\theta_2)]}, \quad (3a)$$

$$S_{33o} = \frac{Z_{ino}-Z_0}{Z_{ino}+Z_0}$$
$$= \frac{-Z_{o2}Z_{o3}\tan(\theta_2)-jZ_0(Z_{o2}+Z_{o3})}{-Z_{o2}Z_{o3}\tan(\theta_2)+jZ_0(Z_{o2}+Z_{o3})}. \quad (3b)$$

Furthermore, by using (3a) and (3b), the scattering parameters of the return loss S_{33} and the insertion loss S_{43} in the Path 2 can be derived as:

$$S_{33} = \frac{S_{11e}+S_{11o}}{2}$$
$$= \frac{Z_{e2}Z_{e3}-jZ_0[Z_{e3}\tan(\theta_2)-Z_{e2}\cot(\theta_2)]}{2Z_{e2}Z_{e3}+j2Z_0[Z_{e3}\tan(\theta_2)-Z_{e2}\cot(\theta_2)]} \quad (4)$$
$$+ \frac{-Z_{o2}Z_{o3}\tan(\theta_2)-jZ_0(Z_{o2}+Z_{o3})}{-2Z_{o2}Z_{o3}\tan(\theta_2)+j2Z_0(Z_{o2}+Z_{o3})},$$

$$S_{43} = \frac{S_{11e}-S_{11o}}{2}$$
$$= \frac{Z_{e2}Z_{e3}-jZ_0[Z_{e3}\tan(\theta_2)-Z_{e2}\cot(\theta_2)]}{2Z_{e2}Z_{e3}+j2Z_0[Z_{e3}\tan(\theta_2)-Z_{e2}\cot(\theta_2)]} \quad (5)$$
$$- \frac{-Z_{o2}Z_{o3}\tan(\theta_2)-jZ_0(Z_{o2}+Z_{o3})}{-2Z_{o2}Z_{o3}\tan(\theta_2)+j2Z_0(Z_{o2}+Z_{o3})}.$$

The ideal situation that the scattering parameter should satisfy at the center frequency is $S_{33}=0$. Thus, (4) can be transformed into Equation (6):

$$Z_0^2(Z_{o2}+Z_{o3})[Z_{e3}\tan^2(\theta_2)-Z_{e2}]$$
$$- Z_{e2}Z_{e3}Z_{o2}Z_{o3}\tan^2(\theta_2) = 0. \quad (6)$$

In addition, if the value of the θ_2 becomes 90°, the scattering parameter of the proposed phase shifter will automatically meet the conditions $S_{33}=0$. Besides, the phase constant ϕ of the Path 2 can be derived from:

$$\tan\phi = \frac{AB(C^2+D^2)-CD(A^2+B^2)}{A^2D^2-B^2C^2}, \quad (7)$$

where

$$A = Z_{e2}Z_{e3}, \quad (8a)$$

$$B = Z_0\left[\frac{Z_{e2}-Z_{e3}\tan^2(\theta_2)}{\tan(\theta_2)}\right], \quad (8b)$$

$$C = Z_{o2}Z_{o3}\tan(\theta_2), \quad (8c)$$

$$D = Z_0(Z_{o2}+Z_{o3}). \quad (8d)$$

Subsequently, considering the reference line (Path 1), the ideal circuit parameters and the phase constant, φ are expressed in [1], in terms of even-mode Z_{e1}, and odd-mode Z_{o1} impedances and its electrical length of the interconnected coupled-line,

$$Z_0 = \sqrt{Z_{e1}Z_{o1}}, \quad (9)$$

and

$$\cos\varphi = \frac{Z_{e1}/Z_{o1}-\tan^2\theta_1}{Z_{e1}/Z_{o1}+\tan^2\theta_1}. \quad (10)$$

Consequently, by combining (7) and (10), the differential phase shift δ between Path 1 and Path 2 for this schematic can be calculated as below:

$$\delta = \angle(S_{43})-\angle(S_{21}) = \tan^{-1}(\phi)-\cos^{-1}(\varphi). \quad (11)$$

For instance, we have assumed that all the electrical lengths of the coupled-lines work under the frequency f_0=2.6 GHz. All the circuit parameters of the proposed typical design parameters can be identified by using Equations (1)-(11). To validate the capability of the proposed broadband phase shifter, five typical examples with the differential shifted phase of 70°, 85°, 100°, 120° and 135° have been designed and simulated.
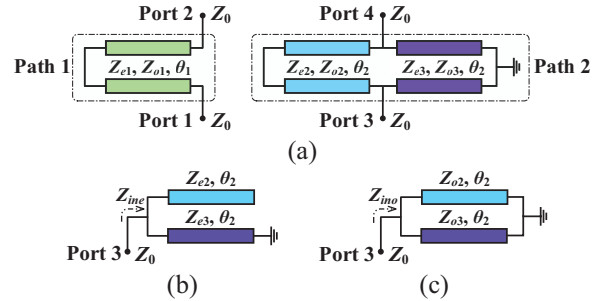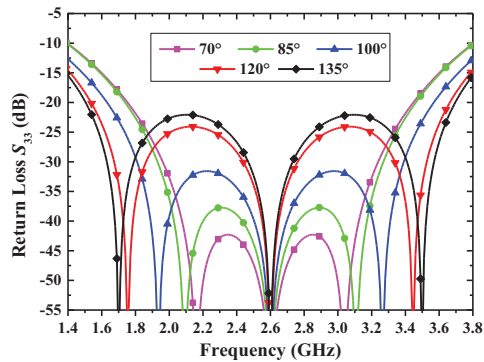

Fig. 1. (a) Circuit configuration of the proposed phase shifter, (b) the even-mode and (c) the odd-mode symmetric equivalent circuit of the Path 2.
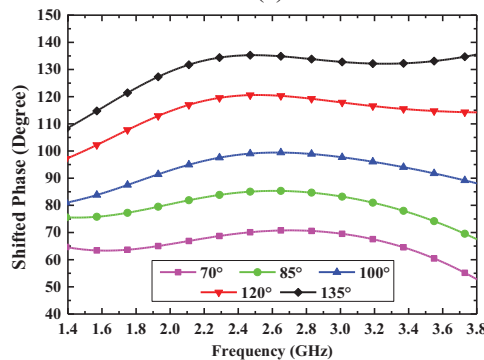
Table 1 lists the corresponding circuit parameters and operating bandwidth in terms of the ideal simulated return losses S_{33} for their amplitude (f_0=2.6 GHz) and phase feature as well, which is also exhibited in Fig. 2. In contrast to [3-6], the proposed structure with a single-layer structure leads to a compact and miniaturized topology, which is easier to be implemented. Meanwhile, it can maintain a wide-band operating properties at a higher frequency band compared with the L/C components in [7].

Table 1: The calculated optimum ideal circuit parameters of five examples for different shifted phase values

Examples	Shifted Phase	Circuit Parameters	Bandwidth (GHz) of |Return Losses| ≤ 10 dB and |phase error| ≤ 5%
I	70°	Z_{e1}=59Ω, Z_{o1}=42.4Ω, Z_{e2}=69Ω, Z_{o2}=60Ω, Z_{e3}=95Ω, Z_{o3}=83Ω, θ_1=121°, θ_2=90°	2.03-3.27 (70°±3.89°)
II	85°	Z_{e1}=59Ω, Z_{o1}=42.4Ω, Z_{e2}=69Ω, Z_{o2}=55Ω, Z_{e3}=95Ω, Z_{o3}=83Ω, θ_1=128°, θ_2=90°	2.03-3.25 (85°±4.72°)
III	100°	Z_{e1}=59Ω, Z_{o1}=42.4Ω, Z_{e2}=69Ω, Z_{o2}=50Ω, Z_{e3}=110Ω, Z_{o3}=90Ω, θ_1=135°, θ_2=90°	2.02-3.34 (100°±5.56°)
IV	120°	Z_{e1}=59Ω, Z_{o1}=42.4Ω, Z_{e2}=69Ω, Z_{o2}=43Ω, Z_{e3}=110Ω, Z_{o3}=90Ω, θ_1=146°, θ_2=90°	1.95-3.85 (120°±6.67°)
V	135°	Z_{e1}=59Ω, Z_{o1}=42.4Ω, Z_{e2}=69Ω, Z_{o2}=43Ω, Z_{e3}=110Ω, Z_{o3}=80Ω, θ_1=154°, θ_2=90°	1.93-3.97 (135°±7.5°)

III. RESULTS AND DISCUSSIONS

To demonstrate the proposed model and theoretical analysis, a 90° broadband phase shifter was simulated, fabricated, and tested as an instance. This circuit was designed on F4B substrate with the relative permittivity of 2.65 and the thickness of 1 mm. Based on the working principle as mentioned before, this instance can be easily realized. The circuit structure of the specified shifted phase and the photograph of the fabricated entity are given in Fig. 3 (a) and Fig. 3 (b). The impedance values of the coupled-lines can be extracted from Equation (1)-(11). The selected characteristic impedances and electrical lengths are as follow: Z_{e1}=59 Ω, Z_{o1}=42.4 Ω, Z_{e2}=70 Ω, Z_{o2}=60 Ω, Z_{e3}=75 Ω, Z_{o3}=50 Ω, θ_1=131° and θ_2=90° at 2.6 GHz. Moreover, for the feasibility of the measurement, the impedance Z_0 of the four ports is defined to 50 Ω. After the line-calculation and optimization of the model, all the physical dimensions are (unit: mm): W_R=2.72, W_1=2.59, W_2=1.7, W_3=1.8, L_1=28.67, L_2=19.8, L_3=19.88, S_1=0.63, S_2=1.8, S_3=0.56 and C=0.4. It should be pointed out that, the size of the interconnected sections at each coupled-line have tiny influence on the performance of the proposed phase shifter due to the simulated process.
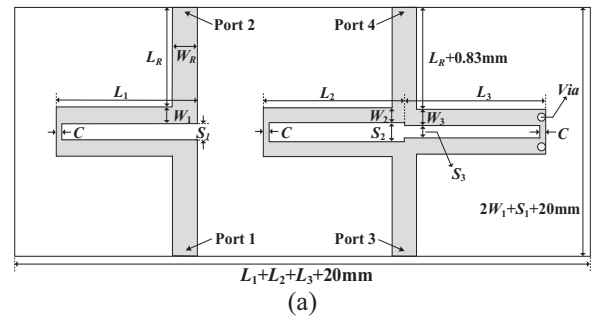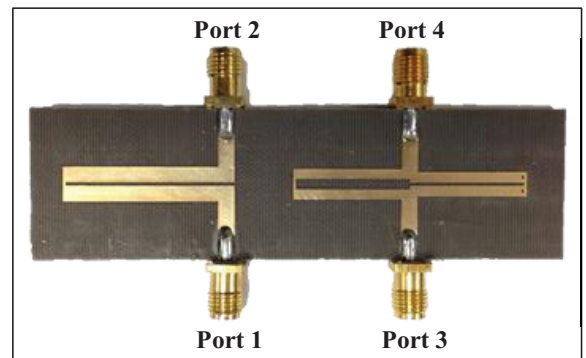

(a)

(b)

Fig. 2. (a) Simulated responses of the proposed phase shifter for the different shifted phase values under the ideal transmission-line models return loss of S_{33}, and (b) different values of shifted phase.

(a)

(b)

Fig. 3. (a) The optimized dimensions, and (b) the photograph of the fabricated 90° phase shifter.

The simulation on the EM model was achieved by HFSS and the measurement was done by an Agilent Network Analyzer. The scattering parameters for both simulation and measurement are exhibited in Fig. 4. A

close agreement between the measurement and the simulation was fulfilled with the return losses better than 10 dB and the insertion losses lower than 0.53 dB (containing the loss imported by SMA connectors). Besides, the operating frequency band can cover a wide bandwidth from 1.34 GHz to 3.20 GHz (over 80%) with a small inaccuracy of shifted phase within $90 \pm 6.7°$. Simultaneously, the main body occupied a miniaturized size smaller in terms of the guided wavelength

$[0.51\lambda_g \times 0.33\lambda_g$ (including port lines), $\lambda_g=77.64$ mm]. In addition, the slight deviation between the simulation and the experiment probably results from simulated algorithm and the calibrated errors from measurement as well. In order to further explain the novelty and advantages of this proposed phase shifter, Tables 2 and 3 summarize the compared characteristics and measured performance between this proposed phase shifter and the other ones in [3-7].
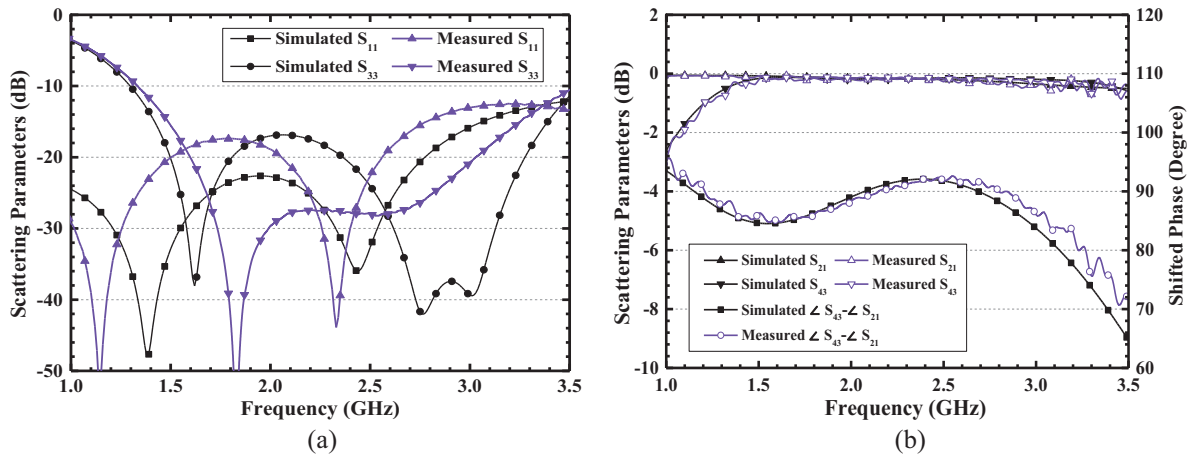

Fig. 4. (a) Simulated and measured results: return losses, and (b) insertion losses and the shifted phase between two outputs of the fabricated 90° phase shifter.

Table 2: The comparison between the proposed phase shifter and previous ones

References	Layer	Type	Symmetry	Substrate	Refer. Line	Main Line	Features	Described Shifting Phases
[3]	Single	Microstrip lines	√	PCB	A 50-Ω transmission line	T-shaped open stub	Easily implemented	60°,75°, 90°,105°, 120°
[4]	Single	Microstrip lines	√	PCB	Phase correcting network using multi-sections of CLs	T-shaped open stub	Complicated, and large size	90°
[5]	Single	Microstrip lines	√	PCB	A 50-Ω transmission line	Multi-section radial stubs and open stub	Inconvenient fabricated and UWB	90°
[6]	Multi-layer	Microstrip patches	×	RO4003C	A 50-Ω transmission line	Broadside-coupled microstrip patches at the top and bottom layer	Inconvenient fabricated, small size and UWB	-180°,-90°, 90°,180°
[7]	Single	L/C components	×	FR4	A 50-Ω transmission line	L/C components	Small size and limitation of higher frequency	22.5°,45°, 90°
This work	Single	Microstrip lines	√	PCB	A pair of coupled-line	Two pair of Coupled-lines	Convenient fabricated, compact and a small size	70°,85°, 100°,120°, 135°

Table 3: The comparison of the measured results between the proposed phase shifter and previous ones

References	Bandwidth (GHz)	Shifting Phase	Phase Error	BW (%)	Return Loss (dB)	Insertion Loss (dB)	Size of Main Body Without Port Line (Wavelength $\lambda_g \times \lambda_g$)
[3]	2.30-5.50	90°	6.4°	82.1	>10	<0.6	0.48×0.35
[4]	2.50-5.43	90°	2.54°	81	>10	<0.8	0.48×0.35
[5]	3.10-10.6	90°	9.02°	109	>10	<0.96	0.81×0.54
[6]	3-11	-180°,-90°,90°,180°	6°,2°,5°,7°	114.3	>10	<0.7,<1.4,<0.6,<1.2	0.2×0.45
[7]	0.58-2.52	90°	5.5°	125	>18.1	<0.16	N. A.
This work	1.34-3.20	90°	6.72°	81.9	>10	<0.53	0.51×0.06

IV. CONCLUSION

This paper reports a novel circuit configuration for the wideband differential phase shifter only comprised of coupled-lines. The circuit of the proposed phase shifter makes it easier to design and fabrication with a compact and miniaturized structure. It can provide a stable shifting phase in a wide bandwidth with low phase deviation. Besides, the theoretical analysis and the various configurations for different shifted phase values are given. For the verification of this novel structure, an example of a broadband 90° phase shifter with coupled-lines was simulated, fabricated, and measured. The measured results validated that it could accomplish a stable wide bandwidth (over 80%) with phase error 90° ± 6.72°, return losses more than 10 dB and low insertion losses less than 0.53 dB. Moreover, the wide-band success with low-cost and miniaturized size of this proposed phase shifter will be of convenience for the combinations of antenna array systems and other microwave systems.

ACKNOWLEDGMENT

REFERENCES

[1] B. Schiffman, "A new class of broadband microwave 90-degree phase shifters," *IRE Trans. Microw. Theory Tech.*, vol. MTT-6, no. 4, pp. 232-237, Apr. 1958.

[2] J. L. R. Quirarte and J. P. Starski, "Novel Schiffman phase shifters," *IEEE Trans. Microw. Theory Tech.*, vol. 41, no. 1, pp. 9-14, Jan. 1993.

[3] S. Y. Zheng, W. S. Chan, and K. F. Man, "Broadband phase shifter using loaded transmission line," *IEEE Microw. Wireless Compon. Lett.*, vol. 20, no. 9, pp. 498-500, Sep. 2010.

[4] S. H. Yeung, T. K. Sarkar, M. Salazar-Palma, and A. Garcia-Lamperez, "A multisection phase correcting network for broadband quadrature power splitter design," *IEEE Microw. Wireless Compon. Lett.*, vol. 23, no. 9, pp. 468-470, Sep.

2013.

[5] S. H. Yeung, Z. Mei, T. K. Sarkar, and M. Salazar-Palma, "Design and testing of a single-layer microstrip ultrawideband 90 differential phase shifter," *IEEE Microw. Wireless Compon. Lett.*, vol. 23, no. 3, pp. 122-124, Mar. 2013.

[6] L. Guo and A. Abbosh, "Phase shifters with wide range of phase and ultra-wideband performance using stub-loaded coupled structure," *IEEE Microw. Wireless Compon. Lett.*, vol. 24, no. 3, pp. 167-169, Mar. 2014.

[7] P.-S. Huang and H.-C. Lu, "Broadband differential phase-shifter design using bridged T-type bandpass network," *IEEE Trans. Microw. Theory Tech.*, vol. 62, no. 7, pp. 1470-1479, July 2014.

[8] J.-S. Hong and M. J. Lancaster, *Microstrip Filters for RF/Microwave Applications*, Wiley, Chapters 1 and 2, 2001.

Yongle Wu received the B.Eng. degree in Communication Engineering and the Ph. D degree in Electronic Engineering from Beijing University of Posts and Telecommunications (BUPT), Beijing, China, in 2006 and 2011, respectively.

During April to October in 2010, he was a Research Assistant at the City University of Hong Kong (CityU), Kowloon, Hong Kong. In 2011, he joined the BUPT. He is currently an Associate Professor with the School of Electronic Engineering, BUPT. His research interests include microwave components and wireless systems design.

Siyue Zhou received the B.Eng. degree in Telecommunications Engineering from Chongqing University of Posts and Telecommunications (CQUPT), China, in 2013, and is currently working toward the Ph.D. degree at Beijing University of Posts and Telecommunications (BUPT), Beijing, China.

Her research interests include microwave components and wireless systems design.

Xiaochuan Shen received the B.Eng. degree in Electronic Information Engineering from Shijiazhuang Tiedao University, China, in 2013, and is currently working toward the Ph.D. degree at Beijing University of Posts and Telecommunications (BUPT), Beijing, China.

His research interests include microwave components and circuits design.

Yuanan Liu received the B.E., M.Eng. and Ph.D. degrees in Electrical Engineering from University of Electronic Science and Technology of China, Chengdu, China, in 1984, 1989 and 1992, respectively.

In 1984, he joined the 26th Institute of Electronic Ministry of China to develop the Inertia Navigating System. In 1992, he began his first post-doctor position in EMC Lab of Beijing University of Posts and Telecommunications (BUPT), Beijing, China. In 1995, he started his second post-doctor in Broadband Mobile Lab of Department of System and Computer Engineering, Carleton University, Ottawa, Canada. From July, 1997, as Professor, he is with Wireless Communication Center of College of Telecommunication Engineering, BUPT, Beijing, China, where he is involved in the development of next-generation cellular system, wireless LAN, Bluetooth application for data transmission, EMC design strategies for high speed digital system, and EMI and EMS measuring sites with low cost and high performance.